

# Kuiper Belt Analogues in Nearby M-type Planet-host Systems

G. M. Kennedy<sup>\*1</sup>, G. Bryden<sup>2</sup>, D. Ardila<sup>3,4</sup>, C. Eiroa<sup>5</sup>, J.-F. Lestrade<sup>6</sup>, J. P. Marshall<sup>7</sup>,  
B. C. Matthews<sup>8,9</sup>, A. Moro-Martin<sup>10</sup>, M. C. Wyatt<sup>11</sup>

<sup>1</sup> Department of Physics, University of Warwick, Gibbet Hill Road, Coventry, CV4 7AL, UK

<sup>2</sup> Jet Propulsion Laboratory, California Institute of Technology, 4800 Oak Grove Drive, Pasadena, CA 91109, USA

<sup>3</sup> NASA Herschel Science Center, California Institute of Technology, MC 100-22, Pasadena, CA 91125, USA

<sup>4</sup> The Aerospace Corporation, M2-266, El Segundo, CA 90245, USA

<sup>5</sup> Dpto. Física Teórica, Universidad Autónoma de Madrid, Cantoblanco, 28049 Madrid, Spain

<sup>6</sup> Observatoire de Paris - LERMA, CNRS, 61 Av. de l'Observatoire, 75014, Paris, France

<sup>7</sup> Academia Sinica, Institute of Astronomy and Astrophysics, Taipei 10617, Taiwan

<sup>8</sup> National Research Council of Canada Herzberg Astronomy & Astrophysics Programs, 5071 West Saanich Road, Victoria, BC, V9E 2E7, Canada

<sup>9</sup> Department of Physics & Astronomy, University of Victoria, 3800 Finnerty Road, Victoria, BC, V8P 5C2, Canada

<sup>10</sup> Space Telescope Science Institute, 3700 San Martin Dr, Baltimore, MD 21218, USA

<sup>11</sup> Institute of Astronomy, University of Cambridge, Madingley Road, Cambridge CB3 0HA, UK

12 November 2021

## ABSTRACT

We present the results of a *Herschel* survey of 21 late-type stars that host planets discovered by the radial velocity technique. The aims were to discover new disks in these systems and to search for any correlation between planet presence and disk properties. In addition to the known disk around GJ 581, we report the discovery of two new disks, in the GJ 433 and GJ 649 systems. Our sample therefore yields a disk detection rate of 14%, higher than the detection rate of 1.2% among our control sample of DEBRIS M-type stars with 98% confidence. Further analysis however shows that the disk sensitivity in the control sample is about a factor of two lower in fractional luminosity than for our survey, lowering the significance of any correlation between planet presence and disk brightness below 98%. In terms of their specific architectures, the disk around GJ 433 lies at a radius somewhere between 1 and 30au. The disk around GJ 649 lies somewhere between 6 and 30au, but is marginally resolved and appears more consistent with an edge-on inclination. In both cases the disks probably lie well beyond where the known planets reside (0.06–1.1au), but the lack of radial velocity sensitivity at larger separations allows for unseen Saturn-mass planets to orbit out to  $\sim 5$ au, and more massive planets beyond 5au. The layout of these M-type systems appears similar to Sun-like star + disk systems with low-mass planets.

**Key words:** planetary systems: formation — circumstellar matter — stars: individual: GJ 433 — stars: individual: GJ 649

## 1 INTRODUCTION

It is now well established that planet formation processes are robust, and proceed around stars of a wide range of masses. At the higher mass end, planets have been discovered around evolved stars with masses up to three times the Sun's (e.g. Setiawan et al. 2005; Johnson et al. 2007b; Reffert et al. 2015). At the lower mass end the results have been equally impressive, with planets discovered around objects ten times less massive than the Sun, and whose luminosity is a thousand times weaker (e.g. Gillon et al. 2016; Anglada-Escudé et al. 2016). This wide mass range provides a unique way to study planet formation

processes, and has shown that while the occurrence rate of giant planets increases towards higher mass stars (Johnson et al. 2007a, 2010a; Reffert et al. 2015), the converse is true for the frequency of Earth to Neptune-mass planets (Mulders et al. 2015).

In tandem with these searches, observations that seek to detect the building blocks of these planets have also been conducted. These mid and far-infrared (IR) surveys detect ‘debris disks’, the collections of small dust particles that are seen to orbit other stars (the ‘dust’ comprises various constituents, such as silicates, ice, and organic compounds). Since their discovery in the 1980's, a growing body of evidence has shown that they can be interpreted as circumstellar disks made up of bodies ranging from  $\sim \mu\text{m}$  to many km in size; while the observations

\* Email: g.kennedy@warwick.ac.uk

only detect  $\mu\text{m}$  to mm-size particles, the lifetime of these particles is commonly shorter than the age of the host star, leading to the conclusion that they must be replenished through the collisional destruction of a mass reservoir of larger planetesimals (e.g. Backman & Paresce 1993). For main-sequence stars this paradigm is generally accepted, so in terms of the dust having an origin in collisions between larger bodies, debris disks can be genuinely thought of as analogues of the Solar System’s Asteroid and Kuiper belts. A key unknown is how the planetesimals acquire high enough relative velocities for their collisions to be destructive; while it is possible that planets excite these velocities (Mustill & Wyatt 2009), it may be a natural outcome upon emergence from the gas rich phase of evolution, or the planetesimals may ‘stir’ themselves (e.g. Kenyon & Bromley 2004), in which case planets are not necessarily needed in order for debris disks to exist.

However, it is well known that the Solar System planets play an important role in sculpting the Asteroid and Kuiper belts, two examples being the presence of the Kirkwood gaps and the capture of Pluto into 2:3 mean motion resonance by Neptune (Malhotra 1993). In attempts to make analogous link in other planetary systems, hypotheses that connect the properties of the disks and planets have been developed, and vary in complexity. The most basic is that some systems are simply ‘better’ at forming large bodies (whether those bodies be planetesimals or planets), and more detailed models suggest that the outcomes depend on whether planetary instabilities occurred (Raymond et al. 2011). As with planets, merely detecting these belts is challenging, so quantifying the connection between the planets and disks in these systems is typically limited to searching for correlations between their basic properties (such as disk brightness, e.g. Kóspál et al. 2009; Bryden et al. 2009; Wyatt et al. 2012; Marshall et al. 2014; Wittenmyer & Marshall 2015; Moro-Martín et al. 2015). Ultimately, these searches yielded a significant correlation between the presence of radial velocity planets and the brightness of debris disks around Sun-like stars (Matthews et al. 2014). This trend is unfortunately not strong, so while splitting the sample to look for trends among sub-samples (e.g. as a function of planet mass) yields tentative trends (e.g. Wyatt et al. 2012) it also lowers the significance. Thus, while there is evidence that some Sun-like stars are indeed better at forming disks and planets than other, the origin of this correlation remains unclear.

In the case of low-mass stars the challenge of finding connections between the planet and disk populations is even greater; for disks at the typical radial distances of a few tens of astronomical units, the low stellar luminosities do not heat the dust to temperatures greater than about 50K. While the Stefan-Boltzmann law therefore limits the luminosity of these disks, the low temperatures further hinder detection because discoveries must be made at far infrared and millimeter wavelengths (e.g. Lestrade et al. 2006, 2012). Thus, it is not particularly surprising that efforts to discover debris disks around late-type stars at mid-infrared wavelengths have often been unsuccessful (e.g. Gautier et al. 2007; Avenhaus et al. 2012). Further, the sensitivity of surveys is normally such that the non-detections are not sufficiently constraining to rule out disks that have similar properties to those that are known to orbit Sun-like stars (Gautier et al. 2007; Morey & Lestrade 2014).

**Table 1.** PACS observations of 16 targets taken as part of our programme (OT2\_gbryden\_2). OD is the Herschel Observing Day, and Repts is the number of repeats of a standard PACS mini scan-map used to reach the desired sensitivity.

Name	ObsIDs	OD	Reps
GJ 176	1342250278/279	1202	6
GJ 179	1342250276/277	1202	6
GJ 317	1342253029/030	1245	6
GJ 3634	1342257175/176	1310	6
GJ 370	1342256997/998	1308	6
GJ 433	1342257567/568	1316	6
GJ 1148	1342247393/394	1138	6
GJ 436	1342247389/390	1138	6
GJ 9425	1342249877/878	1194	6
GJ 9482	1342248728/729	1170	6
HIP 79431	1342262219/220	1355	6
GJ 649	1342252819/820	1244	6
GJ 1214	1342252011/012	1237	6
GJ 674	1342252841/842	1244	6
GJ 676 A	1342243794/795	1058	6
GJ 849	1342246764/765	1121	6

In this paper, we present far infrared *Herschel*<sup>1</sup> (Pilbratt et al. 2010) observations that aim to detect Kuiper belt analogues around a sample of 21 nearby late K and M-type stars that host planets discovered by the radial velocity technique. The primary aim is to search for a correlation between the presence of planets and the brightness of disks, and secondary aims are to detect new disks that may be amenable to further detailed investigation, and to obtain more sensitive observations than were possible with larger surveys. We present the sample and observations in section 2, discuss the results in section 3, and summarise and conclude in section 4.

## 2 SAMPLE AND OBSERVATIONS

Our sample comprises nearly all low-mass planet-host stars within 20pc. Most stars are M spectral type, but we include three that are late K types (GJ 370, GJ 9425 and GJ 9482). Not all systems in the final sample were known to host planets at the time the observations were proposed (2011 September), but some in which planets were subsequently discovered were observed by the volume-limited DEBRIS Key Programme (Matthews et al. 2010). The final sample has 21 stars, 16 of which were observed by *Herschel* in this programme, and which are listed in Table 1. Five more targets, GJ 15 A, GJ 581, GJ 687, GJ 842, and GJ 876, were observed by the DEBRIS survey so are also included in our sample (see Lestrade et al. 2012, for results for GJ 581).

The sample does not include the planet host Proxima Centauri (Anglada-Escudé et al. 2016), as it was not observed by *Herschel*. While it has been suggested to host excess emission arising from a debris disk (Anglada et al. 2017), these observations use the Atacama Large Millimeter Array (ALMA) and this system is therefore not easily integrated into our sample. Two of our targets are possible wide binaries; GJ 15 A (NLTT 919) is

<sup>1</sup> *Herschel* is an ESA space observatory with science instruments provided by European-led Principal Investigator consortia and with important participation from NASA

a common proper motion pair at a projected separation of  $35''$  with NLTT 923 (Gould & Chanamé 2004), and GJ 676 A has a wide common proper motion companion (GJ 676 B) at a projected separation of  $50''$  (Poveda et al. 1994). We do not expect the planetary systems to be affected seriously by these companions, so retain them in our sample.

The targets were observed using the Photodetector Array Camera and Spectrometer (PACS, Poglitsch et al. 2010), using the so-called ‘mini-scan map’ mode. A series of ten parallel scans with a separation of  $4''$  are taken to make a single map, which is repeated six times to build up the signal. One such sequence corresponds to a single observation ID number, or ObsID. The observatory is then rotated by  $40^\circ$ , and the sequence repeated, to provide some robustness to striping artefacts and low-frequency noise. The total integration time for each source is 56 minutes. For our observations the noise level at  $100\mu\text{m}$  was typically 1mJy, while observations carried out by DEBRIS (integration time of 15 minutes) had fewer repeats and a noise level nearer 2mJy. The images used in the analysis are the standard ‘level 2.5’ observatory products obtained from the Herschel Science Archive,<sup>2</sup> which combine the two observing sequences (ObsIDs) into a single image.

Photometry  $F_{\text{obs}}$  for each source was extracted using point spread function (PSF) fitting. Observations of the calibration star  $\gamma$  Dra, again level 2.5 observatory products, were used as PSFs, which were rotated to a position angle appropriate for each observation. The fitting was done at 100 and  $160\mu\text{m}$  simultaneously, so the four free parameters in each fit were a position common to both wavelengths, and two fluxes (i.e.  $F_{100}$  and  $F_{160}$ ). Uncertainties  $\sigma_{100}$  and  $\sigma_{160}$  were estimated by measuring the flux in apertures at hundreds of random locations near the center of the images; this method was found to be more reliable and provide more realistic flux distributions than attempting to fit PSFs at random locations. The apertures were chosen to be those optimal for source extraction ( $5$  and  $8''$  for 100 and  $160\mu\text{m}$  respectively, derived using calibration observations). In the case of GJ 649 there is evidence that the source (i.e. disk) is marginally resolved (see Figure 1), so the flux for this source at  $100\mu\text{m}$  is measured using an aperture radius of  $10''$ , and the uncertainty estimated as above but with  $10''$  apertures. The results of the source extraction are summarised in Table 2, and the results for a few problematic sources are described in more detail below.

To assess whether each star shows the infrared excess that is indicative of a debris disk requires an estimate of the flux density expected from the stellar photosphere  $F_*$  at the PACS wavelengths. These estimates are made by fitting stellar photosphere models to optical and near-IR photometry. The method has been described elsewhere, and for example has been used for the DEBRIS survey and shown to provide photospheric fluxes that are sufficiently precise that the detection of excesses is limited by the *Herschel* photometry, not the photosphere models (i.e.  $\sigma_{\text{obs}} > \sigma_*$ , Kennedy et al. 2012b,a). While photospheric models for late-type stars are less precise than for earlier types (e.g. because of uncertain molecular opacity), the flux of many of our target stars is predicted to be near our noise level and the models are not a limiting factor. The photospheric predictions at 100 and  $160\mu\text{m}$  are given in Table 2.

The significance of any excess is then given in each PACS

bandpass by  $\chi = (F_{\text{obs}} - F_*)/\sqrt{\sigma_{\text{obs}}^2 + \sigma_*^2}$ , where  $\chi > 3$  is taken to be a significant excess. To summarise the observational results; in addition to the disk known to orbit GJ 581, we find two new systems that show strong evidence for infrared excesses: GJ 433 and GJ 649, whose images are shown in Figure 1.

Several other targets were also found to have emission at or near the source position, but in these cases we do not believe the emission to be associated with the star in question. These are shown in Figure 1.

- GJ 3634: A bright ( $\sim 14\text{mJy}$ ) source is seen  $6''$  SW of the expected position of GJ 3634. This offset is larger than expected given the  $\sim 2''$   $1\sigma$  pointing accuracy of *Herschel*<sup>3</sup> and our small sample size. By comparing the positions of several other sources detected in the  $100\mu\text{m}$  PACS image with the (optical) DSS2 plates<sup>4</sup> we found that three were almost perfectly coincident. Thus, we conclude that the  $6''$  offset seen is real, and that the PACS detection near GJ 3634 is not associated with this star.

- HIP 79431: Extended structure is seen to the North of the stellar position, but the peak is  $5''$  away. Only one low S/N source was seen to be common between the PACS and DSS2 images, with perfect coincidence. The background as seen in IRAS and WISE images is complex and variable. We conclude that the large offset and high background mean that the detected source is unlikely to be associated with HIP 79431.

- GJ 674: The background level around GJ 674 is significantly above zero. At  $100\mu\text{m}$  the flux in the image peaks at the position of GJ 674, but if a point source with the photospheric flux of GJ 674 is subtracted the background becomes uniform. Thus, we conclude that the image shows emission from the star GJ 674 superimposed on a non-negligible background, and that there is no evidence for excess emission from the star itself.

### 3 DISCUSSION

Our survey finds two new excess detections, around the stars GJ 433 and GJ 649. We first consider these detections as part of our sample, and then take a closer look at the architecture of these two systems in more detail.

#### 3.1 Planet - disk correlation

One of our goals was to test for a correlation between the brightness of debris disks around low-mass stars and the presence of planets. That is, all stars may host debris disks, but we can only detect those above a given dust level, so we cannot test for a correlation between the ‘existence’ of planets and disks. The same is true for planet detection of course, so we are in fact testing for a correlation between disks above a given brightness threshold and planets above a given semi-major axis vs. mass threshold (acknowledging that the star-to-star sensitivity also varies). These thresholds are discussed below.

A significant correlation has been seen among Sun-like stars that host radial velocity planets (Matthews et al. 2014), and tentative evidence that this trend is stronger for stars that host low-mass planets was found among a small sample of nearby stars (Wyatt et al. 2012; Marshall et al. 2014). No clear trends

<sup>2</sup> <http://archives.esac.esa.int/hsa/whsa/>

<sup>3</sup> <http://herschel.esac.esa.int/Docs/Herschel/html/ch02s04.html>

<sup>4</sup> <https://archive.stsci.edu/dss/>

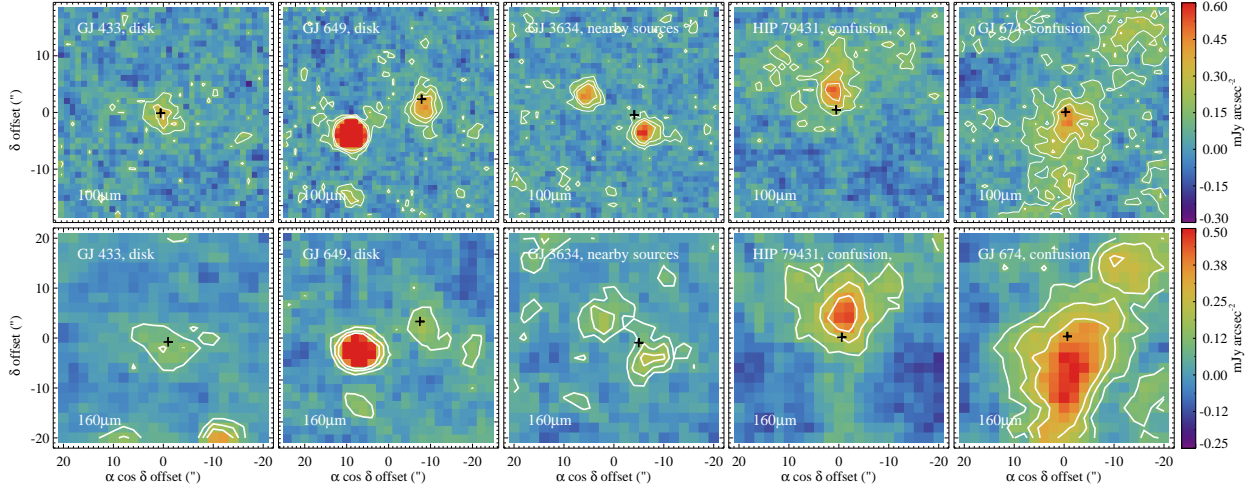


**Figure 1.** *Herschel* images of the two targets found here to host debris disks (GJ 433 and GJ 649, in the left two columns), and the three targets for which excess emission near the star was seen, but which was assumed not to be associated with the star in question (right three columns). In each panel the black cross marks the estimated stellar position at the time of observation. Each image is centered either on the star, or in the case of GJ 649 and GJ 3634 between the two visible source detections. White contours are at 2, 4, and 6 times the  $1\sigma$  noise level in each image. The disk around GJ 649 appears to be marginally resolved; see Figure 4.

**Table 2.** The 21 stars in our sample, comprising 16 stars observed in programme OT2\_gbryden\_2, and five stars observed in programme KPOT\_bmatthew\_1 (DEBRIS): GJ 15, GJ 581 (multiple observations, see Lestrade et al. 2012), GJ 687, GJ 832, and GJ 876. We have not reported flux densities for the two strongly confused sources, HIP 79431 and GJ 674.

GJ	HIP no.	SpTy	Dist (pc)	$F_{*,100}$ (mJy)	$F_{100}$ (mJy)	$\sigma_{100}$ (mJy)	$\chi_{100}$	$F_{*,160}$ (mJy)	$F_{160}$ (mJy)	$\sigma_{160}$ (mJy)	$\chi_{160}$	Notes
GJ 15 A	1475	M2V	3.6	15.3	14.9	2.2	-0.2	5.9	13.2	3.0	2.4	Photosphere at $100\mu\text{m}$
GJ 176	21932	M2.5V	9.4	4.1	3.6	1.6	-0.3	1.6	-3.6	6.4	-0.8	No detection
GJ 179	22627	M2V	12.4	1.3	-1.6	1.2	-2.5	0.5	-4.7	2.8	-1.9	No detection
GJ 317	-	M3.5V	15.3	1.1	3.2	1.1	1.9	0.4	4.9	2.2	2.0	No detection
GJ 370	48331	K6Vk:	11.3	5.7	6.9	0.9	1.3	2.2	-5.2	3.2	-2.3	Photosphere at $100\mu\text{m}$
GJ 3634	-	M2.5	19.8	0.7	-0.9	1.2	-1.3	0.3	3.0	2.8	1.0	Detection at $6''$ SW
<b>GJ 433</b>	56528	M2V	9.1	3.9	11.9	1.3	6.2	1.5	13.9	4.3	2.9	Excess detection
GJ 1148	57050	M4.0Ve	11.1	1.5	1.4	1.0	-0.1	0.6	-2.1	3.3	-0.8	No detection
GJ 436	57087	M3V	9.7	2.4	3.4	1.1	0.9	0.9	4.3	2.3	1.5	No detection
GJ 9425	63833	K9Vk:	15.9	3.1	-0.7	2.1	-1.8	1.2	-15.1	7.6	-2.1	No detection
GJ 9482	70849	K7Vk	23.6	1.0	1.6	1.4	0.5	0.4	-4.1	3.4	-1.3	No detection
GJ 581	74995	M3V	6.3	3.8	21.8	1.5	11.8	1.5	22.4	5.0	4.2	Excess Lestrade et al. (2012)
-	79431	M3V	14.4	1.7	-	-	-	0.6	-	-	-	Extended detection at $5''$ N
<b>GJ 649</b>	83043	M2V	10.4	3.6	22.6	2.4	7.9	1.4	16.3	5.2	2.9	Excess detection, extended?
GJ 1214	-	M4.5V	14.6	0.3	0.9	1.1	0.6	0.1	-0.1	2.3	-0.1	No detection, source $10''$ W
GJ 674	85523	M3V	4.5	8.1	-	-	-	3.1	-	-	-	Extended, high background
GJ 676 A	85647	M0V	15.9	2.6	0.9	1.1	-1.6	1.0	0.5	2.2	-0.2	No detection, source $10''$ SW
GJ 687	86162	M3.0V	4.5	10.1	6.1	1.6	-2.5	3.9	0.2	3.4	-1.1	No detection
GJ 832	106440	M2/3V	5.0	10.4	12.5	1.6	1.3	4.0	1.2	3.5	-0.8	Photosphere at $100\mu\text{m}$
GJ 849	109388	M3.5V	8.8	4.3	4.2	1.2	-0.1	1.7	3.6	1.8	1.1	No detection
GJ 876	113020	M3.5V	4.7	8.1	6.5	1.6	-1.0	3.2	6.5	3.5	0.9	Photosphere at $100\mu\text{m}$

were seen in the volume-limited DEBRIS FGK-type sample considered by Moro-Martín et al. (2015), illustrating the tentative nature of the latter trend, and that samples that do not specifically target planet-host stars suffer from small numbers of planet hosts that limit the power to discover trends.

Here, our sample comprises 21 planet-hosting low-mass stars that were observed in search of IR excesses by *Herschel*, for which three were found to host disks. Thus, our detection rate is 14%, but clearly suffers from a small number

of detections. As a control sample, we consider the volume-limited DEBRIS M-type sample, which comprises 89 nearby stars (Phillips et al. 2010). Of these, two were discovered to host debris disks; the planet host GJ 581 (Lestrade et al. 2012) and the third star in the very wide Fomalhaut triple system, Fomalhaut C (Kennedy et al. 2014). We remove GJ 581 and the four other planet-host stars from this sample, leaving 84 stars with one disk detection, a rate of 1.2%.

A Fisher’s exact test to determine whether these two popu-

lations could arise from the same underlying distribution yields a  $p$ -value of 0.025, thus showing reasonable evidence that the planet-host stars have a tendency to have more detectable (i.e. brighter) debris disks. The Fomalhaut system is known to be relatively young, at 440Myr (Mamajek 2012); if we were to assume that all of the planet host systems are older than this and exclude Fomalhaut C from the control sample the  $p$ -value decreases to 0.01. However, we cannot be sure that the planet-host stars are all older than the Fomalhaut system, since for example GJ 674 may also be a relatively young system (Bonfils et al. 2007).

Thus, we find suggestive evidence that debris disks are more easily detected around M-type stars that also host planets. A further consideration however is whether the observations are biased towards detections for the planet-host sample. This might be expected given that our noise level is about half that of the DEBRIS observations of the control sample, but might also be balanced by the fact that all DEBRIS M-type stars are within 10pc, and thus on average closer than our planet-host stars.

The relative sensitivities for the two samples is shown in Figure 2, where the grey scale shows the number of systems for which disks at a given temperature and above a certain fractional luminosity ( $f = L_{\text{disk}}/L_*$ ) could have been detected. The lowest red contour shows the maximum sensitivity (disks that could have been detected around only one star), the highest shows the level above which disks could have been detected around all stars, and the intermediate contours show where disks could have been detected around 25, 50, and 75% of systems. By comparing the red contours it can be seen that our observations could typically detect disks that are a factor of two to three lower in fractional luminosity than those observed by DEBRIS (as expected from observations that are 2-3 times deeper). While the three disks around planet-host stars could have been detected around 75% of our sample, they could only have been detected around about 30% of the DEBRIS sample. Thus, the evidence for any correlation between planets and debris disk brightness is weaker than suggested by the  $p$ -value above.

The significance of the  $p$ -value may be further reduced by future radial velocity observations, because an implicit assumption is that the stars in the control sample do not host planets in a similar parameter space range as those around our planet-host sample. This is unlikely to be true because not all systems in our control sample will have been observed in search of planets, and our control sample is best termed ‘stars with no known planets’. If any of the systems in the control sample that do not host disks were in fact found to host planets, the significance of our result would decrease further. If however Fomalhaut C were found to host a planet (and a search may be well motivated by our results), the significance would increase.

As noted earlier, it is not yet known whether M-type stars host a disk population that is the same or different to those that orbit Sun-like stars, and a major problem is that obtaining comparably sensitive observations is challenging. This sensitivity difference can be seen by comparing the contours in the right panel of Figure 2 with those in Figure 4 of Sibthorpe et al. (2017, MNRAS in press), which shows the sensitivity for FGK-type stars observed as part of the DEBRIS survey (and for which an FGK-type disk detection rate of 17% was obtained). The 50% contour for our survey is at best about  $f = 5 \times 10^{-6}$ , an order of magnitude better than achieved by DEBRIS for M-type stars. In comparison, our survey is about midway between the two in terms of sensitivity. Therefore, with the caveats that

the number of detections is small, and that the results could be biased by a planet-disk correlation, the fact that we have here obtained a disk detection rate similar to that seen for Sun-like stars suggests that in surveys of equal sensitivity in fractional luminosity the disk detection rate among Sun-like and M-type stars should be approximately the same.

### 3.2 A marginally resolved disk around GJ 649

GJ 649 (HIP 83043, BD+25 3173, LHS 3257) was reported to host a planet with a minimum mass similar to Saturn’s, in an eccentric 598 day (1.1au) orbit (Johnson et al. 2010b). The age of the star is uncertain, though it was classed as a member of the ‘old disk’ (as opposed to the young disk or halo) based on kinematics (Leggett 1992), and noted to be among the 20% most chromospherically active early M-type stars (Johnson et al. 2010b). Using constraints from the disk temperature and *Herschel* images we can therefore build a picture of the system’s architecture.

The flux density distribution for GJ 649 is shown in Figure 3. The excess flux above the photosphere is modelled using a modified blackbody function, where the disk spectrum is divided by  $\lambda/210\mu\text{m}$  beyond  $210\mu\text{m}$ . This steeper long-wavelength spectral slope approximates the poor efficiency of dust emission at wavelengths longer than the grain size, though in this case is not constrained and included simply in order to make the extrapolations to millimeter wavelengths more realistic. The main point to take away from this figure is that the dust thermal emission is very cold, so could not have been detected in the WISE observations at  $22\mu\text{m}$ . The best-fit disk temperature is 50K with  $f = 7 \times 10^{-5}$ , but is uncertain because the  $160\mu\text{m}$  observation is not formally a  $3\sigma$  detection of the disk (i.e. Table 2 shows that  $\chi_{160}$  for GJ 649 is 2.9). The non-detection of an excess at  $22\mu\text{m}$  means that the temperature cannot be significantly more than 100K.

Given a stellar luminosity of  $0.044L_{\odot}$  the best fit temperature of 50K corresponds to a radial distance of 6au if the disk material behaves as a blackbody, while a temperature of 100K yields a distance of about 2au. Given that most debris disks are comprised of dust small enough to have super-blackbody temperatures, the disk around GJ 649 would be expected to be larger than blackbody estimates, by a factor of several at least (e.g. Rodriguez & Zuckerman 2012; Booth et al. 2013; Pawellek et al. 2014; Morales et al. 2016). This factor was found to be 6-20 for GJ 581 (Lestrade et al. 2012), with the large uncertainty arising because the disk radius depends on the square of the temperature. At a distance of 10.4pc (Lindegren et al. 2016) the GJ 649 disk may therefore have an angular diameter large enough to be resolved. This extent may be confirmed by the *Herschel* images, which at  $100\mu\text{m}$  show some extended residual emission after PSF subtraction (see Figure 4). The fact that these residuals are extended in a non-axisymmetric pattern suggests that the disk may be nearer to edge-on than face-on, as might be expected given in the case of a planet detection with the radial velocity technique. Given that most of the residual contours are only  $1\sigma$  however, we consider that these residuals provide circumstantial evidence that the disk is resolved, in which case the disk diameter would be similar to the PACS beam size of  $6''$ . We therefore conclude that the disk radius could lie in the range 2-50au, but is more likely to be a few tens of au.

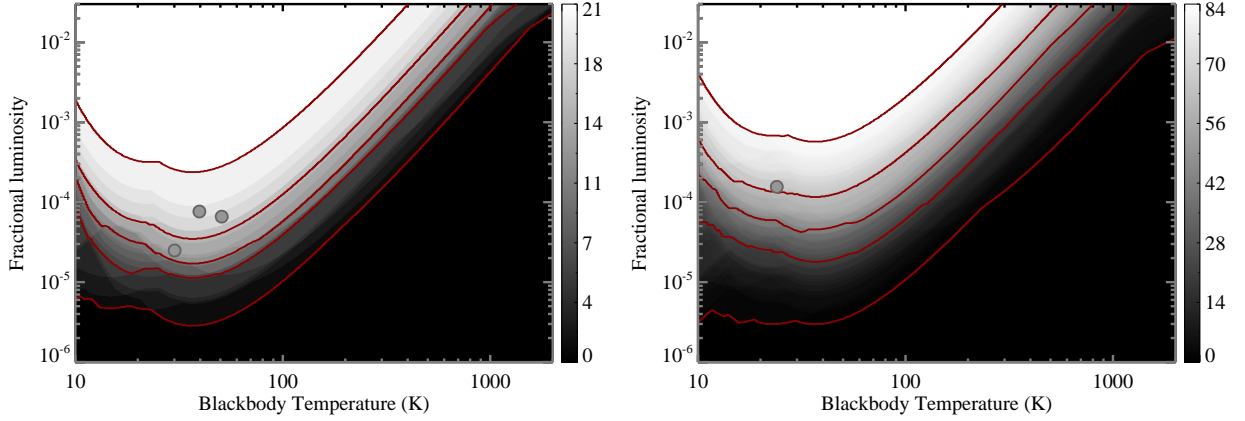


**Figure 2.** Detection space for our sample (*left panel*) and the control sample (*right panel*). Contours show the number of stars for which a disk of a given fractional luminosity and temperature could have been detected. The upper and lower red contours show where disks around all, and one, systems could have been detected. The intermediate curves are for 75, 50, and 25% of systems. The difference in sensitivity between our sample and the DEBRIS control sample is a factor of a few.

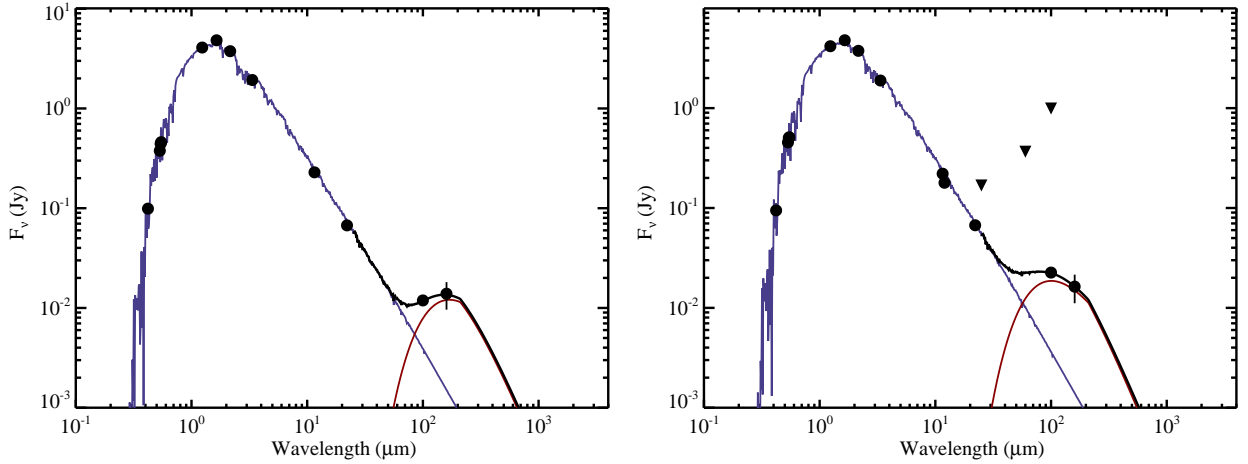


**Figure 3.** Flux distributions showing the disk detections for GJ 433 (*left panel*) and GJ 649 (*right panel*). Solid lines show the star (blue), disk (red), and total (black) models. Black dots and triangles show measured photometry and upper limits. The best fit disk temperatures are 30 and 50K, though the large uncertainties in the 160 $\mu$ m measurements make these very uncertain.

The system layout is shown in Figure 5, where the planet GJ 649 b is indicated by the dot, and the error bar indicates the range of radii covered by the eccentric orbit. The solid line shows limits estimated based on the radial velocity residuals once the best-fit planet orbit is subtracted,<sup>5</sup> indicating that planets more massive than Saturn that orbit beyond about 5au would not have been detected. The range of estimated disk locations is shown by the hatched region, where we have taken the marginally resolved image to indicate that the disk has a radius between 10-30au. The basic conclusion is that while the separation between the planet and disk is probably large, it is possible

<sup>5</sup> The inner part of this limit can be derived using Kepler’s laws and the residual noise in the RV data once the planet(s) have been subtracted, but the steeper outer part where the orbital period is longer than the span of observations was empirically estimated from full simulations of radial velocity sensitivity (e.g. Kennedy et al. 2015)

that this gap is occupied by one or more undetected planets. A further conclusion is that lower mass planets at smaller radii could have been detected, though the sensitivity is a factor of two poorer than for the other systems discussed below.

### 3.3 An unresolved disk around GJ 433

GJ 433 (HIP 56528, LHS 2429) was reported to host a low-mass planet GJ 433 b ( $M \sin i = 5.8M_{\oplus}$ ) on a 7.4 day period at 0.058 au (Delfosse et al. 2013). They detected an additional significant signal with a much longer period of 10 years (3.6au), but based on the variation of activity indices on a similar timescale (Gomes da Silva et al. 2011), concluded that a magnetic cycle of the star was a more likely origin. The same signals were recovered by Tuomi et al. (2014), who considered the second signal to be a candidate planet. Given the uncertain nature of the outer planet we do not include it here. The age of GJ 433 is uncertain, but the dynamical, x-ray, and Ca II emis-

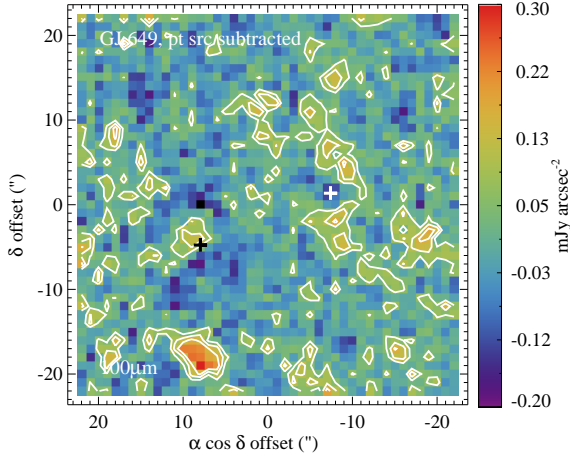


**Figure 4.** *Herschel* image of GJ 649 after subtracting point sources near the location of GJ 649 (at the white +) and at the bright peak to the SE (at the black +, see Figure 1). The low level residual structure around GJ 649 provides circumstantial, though not conclusive, evidence, that the disk is resolved. The asymmetry in the residuals suggests that the disk position angle is near to North, and that the disk is closer to edge-on than face-on. White contours are at 1, 2, and 3 times the  $1\sigma$  noise level. The center of the image is approximately midway between the plus symbols.

sion properties show that the star is not young (Delfosse et al. 2013).

As above we can constrain the disk location relative to the planet’s, but in the case of GJ 433 there is no clear evidence that the disk is resolved with *Herschel*. The best fit disk temperature is 30K (see Figure 3, but again the temperature is poorly constrained by a weak detection at  $160\mu\text{m}$ , and could be as warm as 100K. The fractional luminosity is also poorly constrained, but is approximately  $2.5 \times 10^{-5}$ . For the stellar luminosity of  $0.033L_{\odot}$  a disk temperature range from 100 to 30K yields a blackbody radius range of about 1 to 16au, or about 0.2 to  $3.5''$  diameter at the 9.1pc distance of the system. As for GJ 649, the disk structure as seen at  $100\mu\text{m}$  can constrain the disk extent to less than the PACS beam size, but as with GJ 649 only limits the disk radius to less than about 30au, and does not constrain the inclination or position angle.

The system layout is shown in Figure 5. While the observational limits on the disk radius are poor, a radius of 1au would make GJ 433 host to an unusually small disk (Wyatt et al. 2007), so it seems most likely that the disk extent is similar to that expected for GJ 649. If this is indeed the case, there is again space for undetected planets in the region between the known planet and the disk.

### 3.4 Summary of system architectures

Figure 5 summarises the architecture of the planet-host systems in our sample, and includes the multi-planet system GJ 581. The number of planets residing in this system is contentious, and stellar activity has been proposed as the cause of some of the periodic signals seen; here we show the three planets proposed by Robertson et al. (2014), and the hatched disk region shows the extent of the disk derived by Lestrade et al. (2012). As with

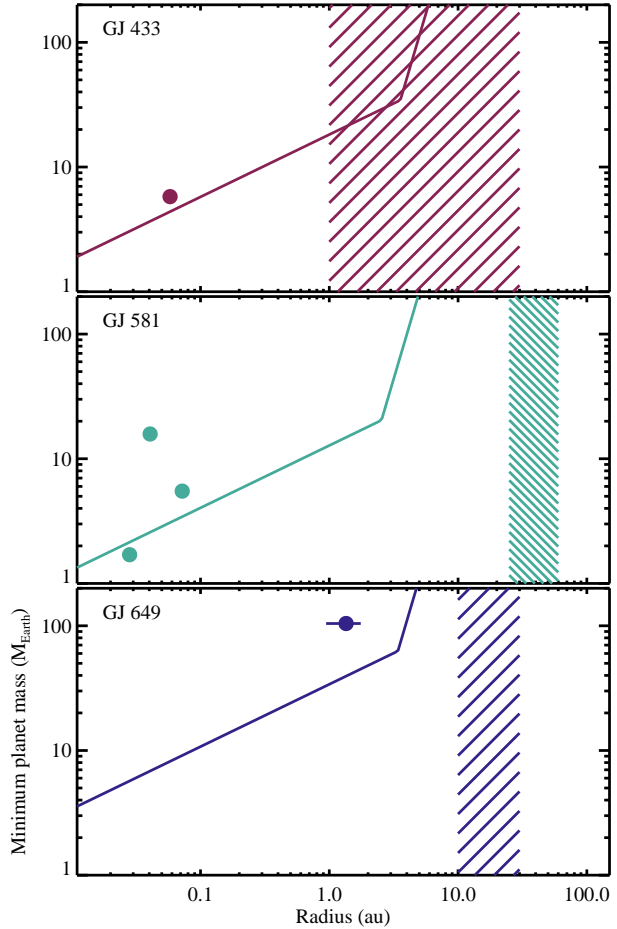


**Figure 5.** Mass semi-major axis diagrams showing the GJ 433, GJ 581, and GJ 649 planets (dots), the approximate RV sensitivity (lines), and the possible range of disk locations (hatched regions), showing the disk extent in the case of GJ 581). GJ 581 e lies below the sensitivity curve because the RV amplitude ( $1.7 \text{ m s}^{-1}$ ) is smaller than the RMS ( $2.12 \text{ m s}^{-1}$ ) reported by Robertson et al. (2014). In each case, with the possible exception of GJ 433, there remains room in the detection space for sizeable planets that reside between the known planets and the disk, but that could not have been detected with the current RV observations.

GJ 433 and GJ 649, there is space for undetected planets in the intervening region.

Given the lack of strong evidence for any correlation between the presence of planets and debris disk brightness, we should not necessarily expect clear trends when looking at plots such as Figure 5. We might however note trends that are glossed over by a simple disk brightness metric, such as tendencies for systems to show particular architectures or scales. Again noting that a disk as small as 1au around GJ 433 would be very unusual, the radii of the disks is consistent with being a few tens of au. However, this size is also inferred for the disk that orbits Fomalhaut C (Kennedy et al. 2014), so there is no evidence that this preference is related to the presence of planets. Indeed, this radius range is also preferred for disks around FGK-stars, independent of whether planets are known (Sibthorpe et al. 2017).

There is no obvious link between the disks and the layout of the planets that orbit closer in, but in each case there remains room in the detection space for sizeable planets that re-

side between the known planets and the disk, but that could not have been detected with the current RV observations. In this regard the M-type planet + disk systems appear to be analogues of Sun-like planet + disk systems such as HD 20794, HD 38858, and 61 Vir (Wyatt et al. 2012; Kennedy et al. 2015). This similarity may however simply reflect that detecting long period planets takes time, and that small debris disks grind down to undetectable levels more rapidly than large ones, and that these biases are present regardless of the mass of the host star. That is, there may be differences in the architectures of planetary systems across different spectral types, but that this difference is in the type or existence of planets that reside near 10au. For further discussion of planet formation scenarios, we refer the reader to Wyatt et al. (2012), Kennedy et al. (2015), and Marino et al. (2017).

The very cool disk temperatures shown in Figure 3 make it clear that progress in our understanding of these disks, and the links with the planets, can only be made by far infrared and millimeter-wave observations. The present observations are hindered by the low spatial resolution of *Herschel*, which means that we are constrained to estimating disk locations. With no far infrared missions on the near horizon, and an expectation of sub-mJy disk flux densities, observations with the Atacama Large Millimeter Array (ALMA) are the main avenue for progress. These will be challenging, but necessary to obtain further discoveries, and in cases such as GJ 433, GJ 581, and GJ 649 could provide higher resolution images that instead of yielding disk location estimates, will allow the discussion of disk structure.

#### 4 CONCLUSIONS

This paper presents the results of a *Herschel* survey of 21 nearby late-type stars that host planets discovered by the radial velocity technique. These observations were obtained with the aim of discovering new debris disks in these systems, and in search of any correlation between planet presence and disk brightness.

We report the discovery of two previously undetected disks, residing at a few tens of au around the stars GJ 433 and GJ 649. The disk around GJ 649 appears marginally resolved and more consistent with being viewed edge-on. Despite uncertainty in their radii these disks orbit well beyond the known planets, and it is possible that other as-yet undetected planets reside in the intervening regions. The layout of these systems therefore appears similar to star + disk systems around Sun-like stars such as HD 20794, HD 38858, and 61 Vir. Estimating the ages of M-type stars is challenging, but neither star shows evidence of youth, so there is no evidence that the ages of these stars are special compared to the rest of the sample.

Including the previously known disk around GJ 581, our sample comprises three planet hosts with disks, a detection rate of 14%. While this rate is higher than for a control sample of M-type stars without reported planets observed by the DEBRIS survey (1 out of 84 stars), the difference is only significant at 98% confidence. This evidence is further shown to be optimistic, because the observations of the planet-host sample were somewhat more sensitive to debris disks than those in the control sample, and because not all systems in the control sample have been searched for planets (or reported not to have planets above some detection threshold).

Though this survey represents an improvement over previ-

ous surveys of M-type stars, the fractional luminosity sensitivity achieved remains about a factor of three poorer than similar surveys of Sun-like stars. Nevertheless, the fact that we find disks around 14% of M-type stars, in comparison to 17% of Sun-like stars, provides circumstantial evidence that there is no difference in their disk populations.

#### 5 ACKNOWLEDGEMENTS

We thank the referee for a useful report. GMK is supported by the Royal Society as a Royal Society University Research Fellow. This work was supported by the European Union through ERC grant number 279973 (GMK & MCW).

The Digitized Sky Survey was produced at the Space Telescope Science Institute under U.S. Government grant NAG W-2166. The images of these surveys are based on photographic data obtained using the Oschin Schmidt Telescope on Palomar Mountain and the UK Schmidt Telescope. The plates were processed into the present compressed digital form with the permission of these institutions.

#### REFERENCES

- Anglada, G., Amado, P. J., Ortiz, J. L., Gómez, J. F., Macías, E., Alberdi, A., Osorio, M., Gómez, J. L., de Gregorio-Monsalvo, I., Pérez-Torres, M. A., Anglada-Escudé, G., Berdiñas, Z. M., Jenkins, J. S., Jimenez-Serra, I., Lara, L. M., López-González, M. J., López-Puertas, M., Morales, N., Ribas, I., Richards, A. M. S., Rodríguez-López, C., & Rodríguez, E. 2017, ArXiv e-prints
- Anglada-Escudé, G., Amado, P. J., Barnes, J., Berdiñas, Z. M., Butler, R. P., Coleman, G. A. L., de La Cueva, I., Dreizler, S., Endl, M., Giesers, B., Jeffers, S. V., Jenkins, J. S., Jones, H. R. A., Kiraga, M., Kürster, M., López-González, M. J., Marvin, C. J., Morales, N., Morin, J., Nelson, R. P., Ortiz, J. L., Ofir, A., Paardekooper, S.-J., Reiners, A., Rodríguez, E., Rodríguez-López, C., Sarmiento, L. F., Strachan, J. P., Tsapras, Y., Tuomi, M., & Zechmeister, M. 2016, *Nature*, 536, 437
- Avenhaus, H., Schmid, H. M., & Meyer, M. R. 2012, *A&A*, 548, A105
- Backman, D. E. & Paresce, F. 1993, in *Protostars and Planets III*, ed. E. H. Levy & J. I. Lunine, 1253–1304
- Bonfils, X., Mayor, M., Delfosse, X., Forveille, T., Gillon, M., Perrier, C., Udry, S., Bouchy, F., Lovis, C., Pepe, F., Queloz, D., Santos, N. C., & Bertaux, J.-L. 2007, *A&A*, 474, 293
- Booth, M., Kennedy, G., Sibthorpe, B., Matthews, B. C., Wyatt, M. C., Duchêne, G., Kavelaars, J. J., Rodríguez, D., Greaves, J. S., Koning, A., Vican, L., Rieke, G. H., Su, K. Y. L., Moro-Martín, A., & Kalas, P. 2013, *MNRAS*, 428, 1263
- Bryden, G., Beichman, C. A., Carpenter, J. M., Rieke, G. H., Stapelfeldt, K. R., Werner, M. W., Tanner, A. M., Lawler, S. M., Wyatt, M. C., Trilling, D. E., Su, K. Y. L., Blaylock, M., & Stansberry, J. A. 2009, *ApJ*, 705, 1226
- Delfosse, X., Bonfils, X., Forveille, T., Udry, S., Mayor, M., Bouchy, F., Gillon, M., Lovis, C., Neves, V., Pepe, F., Perrier, C., Queloz, D., Santos, N. C., & Ségransan, D. 2013, *A&A*, 553, A8

- Gautier, III, T. N., Rieke, G. H., Stansberry, J., Bryden, G. C., Stapelfeldt, K. R., Werner, M. W., Beichman, C. A., Chen, C., Su, K., Trilling, D., Patten, B. M., & Roellig, T. L. 2007, *ApJ*, 667, 527
- Gillon, M., Jehin, E., Lederer, S. M., Delrez, L., de Wit, J., Burdanov, A., Van Grootel, V., Burgasser, A. J., Triaud, A. H. M. J., Opitom, C., Demory, B.-O., Sahu, D. K., Bardalez Gagliuffi, D., Magain, P., & Queloz, D. 2016, *Nature*, 533, 221
- Gomes da Silva, J., Santos, N. C., Bonfils, X., Delfosse, X., Forveille, T., & Udry, S. 2011, *A&A*, 534, A30
- Gould, A. & Chanamé, J. 2004, *ApJS*, 150, 455
- Johnson, J. A., Aller, K. M., Howard, A. W., & Crepp, J. R. 2010a, *PASP*, 122, 905
- Johnson, J. A., Butler, R. P., Marcy, G. W., Fischer, D. A., Vogt, S. S., Wright, J. T., & Peek, K. M. G. 2007a, *ApJ*, 670, 833
- Johnson, J. A., Fischer, D. A., Marcy, G. W., Wright, J. T., Driscoll, P., Butler, R. P., Hekker, S., Reffert, S., & Vogt, S. S. 2007b, *ApJ*, 665, 785
- Johnson, J. A., Howard, A. W., Marcy, G. W., Bowler, B. P., Henry, G. W., Fischer, D. A., Apps, K., Isaacson, H., & Wright, J. T. 2010b, *PASP*, 122, 149
- Kennedy, G. M., Matrà, L., Marmier, M., Greaves, J. S., Wyatt, M. C., Bryden, G., Holland, W., Lovis, C., Matthews, B. C., Pepe, F., Sibthorpe, B., & Udry, S. 2015, *MNRAS*, 449, 3121
- Kennedy, G. M., Wyatt, M. C., Kalas, P., Duchêne, G., Sibthorpe, B., Lestrade, J.-F., Matthews, B. C., & Greaves, J. 2014, *MNRAS*, 438, L96
- Kennedy, G. M., Wyatt, M. C., Sibthorpe, B., Duchêne, G., Kalas, P., Matthews, B. C., Greaves, J. S., Su, K. Y. L., & Fitzgerald, M. P. 2012a, *MNRAS*, 421, 2264
- Kennedy, G. M., Wyatt, M. C., Sibthorpe, B., Phillips, N. M., Matthews, B. C., & Greaves, J. S. 2012b, *MNRAS*, 426, 2115
- Kenyon, S. J. & Bromley, B. C. 2004, *AJ*, 127, 513
- Kóspál, Á., Ardila, D. R., Moór, A., & Ábrahám, P. 2009, *ApJ*, 700, L73
- Leggett, S. K. 1992, *ApJS*, 82, 351
- Lestrade, J.-F., Matthews, B. C., Sibthorpe, B., Kennedy, G. M., Wyatt, M. C., Bryden, G., Greaves, J. S., Thilliez, E., Moro-Martín, A., Booth, M., Dent, W. R. F., Duchêne, G., Harvey, P. M., Horner, J., Kalas, P., Kavelaars, J. J., Phillips, N. M., Rodriguez, D. R., Su, K. Y. L., & Wilner, D. J. 2012, *A&A*, 548, A86
- Lestrade, J.-F., Wyatt, M. C., Bertoldi, F., Dent, W. R. F., & Menten, K. M. 2006, *A&A*, 460, 733
- Lindgren, L., Lammers, U., Bastian, U., Hernández, J., Klioner, S., Hobbs, D., Bombrun, A., Michalik, D., Ramos-Lerate, M., Butkevich, A., Comoretto, G., Joliet, E., Holl, B., Hutton, A., Parsons, P., Steidelmüller, H., Abbas, U., Altmann, M., Andrei, A., Anton, S., Bach, N., Barache, C., Beciani, U., Berthier, J., Bianchi, L., Biermann, M., Bouquillon, S., Bourda, G., Brüsemeister, T., Bucciarelli, B., Busonero, D., Carlucci, T., Castañeda, J., Charlot, P., Clotet, M., Crosta, M., Davidson, M., de Felice, F., Drimmel, R., Fabricius, C., Fienga, A., Figueras, F., Fraile, E., Gai, M., Garralda, N., Geyer, R., González-Vidal, J. J., Guerra, R., Hambly, N. C., Hauser, M., Jordan, S., Lattanzi, M. G., Lenhardt, H., Liao, S., Löffler, W., McMillan, P. J., Mignard, F., Mora, A., Morbidelli, R., Portell, J., Riva, A., Sarasso, M., Serraller, I., Sidiq, H., Smart, R., Spagna, A., Stampa, U., Steele, I., Taris, F., Torra, J., van Reeve, W., Vecchiato, A., Zschocke, S., de Bruijne, J., Gracia, G., Raison, F., Lister, T., Marchant, J., Messineo, R., Soffel, M., Osorio, J., de Torres, A., & O'Mullane, W. 2016, *A&A*, 595, A4
- Malhotra, R. 1993, *Nature*, 365, 819
- Mamajek, E. E. 2012, *ApJ*, 754, L20
- Marino, S., Wyatt, M. C., Kennedy, G. M., Holland, W., Matrà, L., Shannon, A., & Ivison, R. J. 2017, *MNRAS*, 469, 3518
- Marshall, J. P., Moro-Martín, A., Eiroa, C., Kennedy, G., Mora, A., Sibthorpe, B., Lestrade, J.-F., Maldonado, J., Sanz-Forcada, J., Wyatt, M. C., Matthews, B., Horner, J., Montesinos, B., Bryden, G., del Burgo, C., Greaves, J. S., Ivison, R. J., Meeus, G., Olofsson, G., Pilbratt, G. L., & White, G. J. 2014, *A&A*, 565, A15
- Matthews, B. C., Krivov, A. V., Wyatt, M. C., Bryden, G., & Eiroa, C. 2014, *Protostars and Planets VI*, 521
- Matthews, B. C., Sibthorpe, B., Kennedy, G., Phillips, N., Churcher, L., Duchêne, G., Greaves, J. S., Lestrade, J.-F., Moro-Martín, A., Wyatt, M. C., Bastien, P., Biggs, A., Bouvier, J., Butner, H. M., Dent, W. R. F., di Francesco, J., Eislöffel, J., Graham, J., Harvey, P., Hauschildt, P., Holland, W. S., Horner, J., Ibar, E., Ivison, R. J., Johnstone, D., Kalas, P., Kavelaars, J., Rodriguez, D., Udry, S., van der Werf, P., Wilner, D., & Zuckerman, B. 2010, *A&A*, 518, L135
- Morales, F. Y., Bryden, G., Werner, M. W., & Stapelfeldt, K. R. 2016, *ApJ*, 831, 97
- Morey, É. & Lestrade, J.-F. 2014, *A&A*, 565, A58
- Moro-Martín, A., Marshall, J. P., Kennedy, G., Sibthorpe, B., Matthews, B. C., Eiroa, C., Wyatt, M. C., Lestrade, J.-F., Maldonado, J., Rodriguez, D., Greaves, J. S., Montesinos, B., Mora, A., Booth, M., Duchêne, G., Wilner, D., & Horner, J. 2015, *ApJ*, 801, 143
- Mulders, G. D., Pascucci, I., & Apai, D. 2015, *ApJ*, 798, 112
- Mustill, A. J. & Wyatt, M. C. 2009, *MNRAS*, 399, 1403
- Pawellek, N., Krivov, A. V., Marshall, J. P., Montesinos, B., Ábrahám, P., Moór, A., Bryden, G., & Eiroa, C. 2014, *ApJ*, 792, 65
- Phillips, N. M., Greaves, J. S., Dent, W. R. F., Matthews, B. C., Holland, W. S., Wyatt, M. C., & Sibthorpe, B. 2010, *MNRAS*, 403, 1089
- Pilbratt, G. L., Riedinger, J. R., Passvogel, T., Crone, G., Doyle, D., Gageur, U., Heras, A. M., Jewell, C., Metcalfe, L., Ott, S., & Schmidt, M. 2010, *A&A*, 518, L1
- Poglitich, A., Waelkens, C., Geis, N., Feuchtgruber, H., Vandenbussche, B., Rodriguez, L., Krause, O., Renotte, E., van Hoof, C., Saraceno, P., Cepa, J., Kerschbaum, F., Agnèse, P., Ali, B., Altieri, B., Andreani, P., Augeres, J.-L., Balog, Z., Barl, L., Bauer, O. H., Belbachir, N., Benedettini, M., Bilot, N., Boulade, O., Bischof, H., Blommaert, J., Callut, E., Cara, C., Cerulli, R., Cesarsky, D., Contursi, A., Creten, Y., De Meester, W., Doublier, V., Doumayrou, E., Duband, L., Exter, K., Genzel, R., Gillis, J.-M., Grözinger, U., Henning, T., Herreros, J., Huygen, R., Inguccio, M., Jakob, G., Jamar, C., Jean, C., de Jong, J., Katterloher, R., Kiss, C., Klaas, U., Lemke, D., Lutz, D., Madden, S., Marquet, B., Martignac, J., Mazy, A., Merken, P., Montfort, F., Morbidelli, L., Müller, T., Nielbock, M., Okumura, K., Orfei, R., Ottensamer, R., Pezzuto, S., Popesso, P., Putzeys, J., Regibo, S., Reveret, V., Royer, P., Sauvage, M., Schreiber, J., Stegmaier, J., Schmitt, D., Schubert, J., Sturm, E., Thiel, M., Tofani, G., Vavrek, R., Wetzstein, M., Wieprecht, E., & Wiezorrek, E. 2010, *A&A*, 518, L2
- Poveda, A., Herrera, M. A., Allen, C., Cordero, G., & Lavalley,

- C. 1994, *Rev. Mexicana Astron. Astrofis.*, 28, 43
- Raymond, S. N., Armitage, P. J., Moro-Martín, A., Booth, M., Wyatt, M. C., Armstrong, J. C., Mandell, A. M., Selsis, F., & West, A. A. 2011, *A&A*, 530, A62
- Reffert, S., Bergmann, C., Quirrenbach, A., Trifonov, T., & Künstler, A. 2015, *A&A*, 574, A116
- Robertson, P., Mahadevan, S., Endl, M., & Roy, A. 2014, *Science*, 345, 440
- Rodriguez, D. R. & Zuckerman, B. 2012, *ApJ*, 745, 147
- Setiawan, J., Rodmann, J., da Silva, L., Hatzes, A. P., Pasquini, L., von der Lühe, O., de Medeiros, J. R., Döllinger, M. P., & Girardi, L. 2005, *A&A*, 437, L31
- Tuomi, M., Jones, H. R. A., Barnes, J. R., Anglada-Escudé, G., & Jenkins, J. S. 2014, *MNRAS*, 441, 1545
- Wittenmyer, R. A. & Marshall, J. P. 2015, *AJ*, 149, 86
- Wyatt, M. C., Kennedy, G., Sibthorpe, B., Moro-Martín, A., Lestrade, J.-F., Ivison, R. J., Matthews, B., Udry, S., Greaves, J. S., Kalas, P., Lawler, S., Su, K. Y. L., Rieke, G. H., Booth, M., Bryden, G., Horner, J., Kavelaars, J. J., & Wilner, D. 2012, *MNRAS*, 424, 1206
- Wyatt, M. C., Smith, R., Greaves, J. S., Beichman, C. A., Bryden, G., & Lisse, C. M. 2007, *ApJ*, 658, 569